Ultralow Power Dissipation Optical Interconnects: Directly Modulated Membrane Lasers and Photonics Crystal Lasers

Koji Takeda(1),(2) and Shinji Matsuo(1),(2)

(1) NTT Device Technology Laboratories, NTT Corporation, koji.takeda.vk@hco.ntt.co.jp
(2) NTT Nanophotonics Center, NTT Corporation

Abstract *Low-power dissipation lasers on Si are needed for short-distance optical interconnects. We review our recent progress on semiconductor lasers ranging from 100-μm long to wavelength-scale cavities. Strong optical confinement and gratings with a large coupling coefficient are the key to attaining ultralow power consumption lasers.*

Introduction

As Internet traffic continues to grow rapidly, the performance of data centres and high-performance computers need to improve as well. Recently, a large number of optical interconnects have been introduced in data centres, and there have been many attempts to introduce optical interconnects for much shorter distances[1-2], e.g., board-to-board, chip-to-chip, and on-chip. To use optical interconnects in such short distances, the energy consumption of each component needs to be reduced[3].

In this context, we have studied energy efficient light sources suitable for short-distance optical interconnects. There are two ways to obtain modulated light: by using continuous-wave lasers and modulators, or by directly modulating lasers. Directly modulated lasers (DMLs) are considered more suitable because of their simple configuration and low energy consumption. The energy consumption of DMLs can be further reduced by minimizing the active volume, which will be discussed in the next section.

In this paper, we report our recent progress on small DMLs suitable for short-distance optical interconnects. The first type of DMLs are membrane lasers that utilize thin III-V-based membranes on SiO_2/Si substrates. The second type are photonic-crystal (PhC) lasers that can further reduce the active volume so that an ultrasmall threshold current and low energy consumption can be attained. To obtain lasing from such small cavities, it is necessary to increase the coupling coefficient of gratings or the quality (Q) factor of PhC. Due to their membrane structures, we were easily able to increase the coupling coefficients so that these lasers could operate as intended.

Device design and fabrication

To reduce the power consumption of a directly modulated laser, the active volume needs to be reduced, as described below. The relaxation oscillation frequency (f_r) of semiconductor lasers is obtained by

$$f_r = \frac{1}{2\pi}\sqrt{\frac{\Gamma v_g}{qV}\frac{dg}{dn}\eta_i\left(I_b - I_{th}\right)}$$

where Γ is the confinement factor in the active region, v_g is the group velocity, dg/dn is the differential gain and V is the active volume[4]. From this equation, it can be understood that in order to reduce power consumption—that is, to operate at a low bias current—it is important to increase the confinement factor (Γ) and decrease the active volume (V). Thus, we used a thin III-V-based membrane on SiO_2/Si.

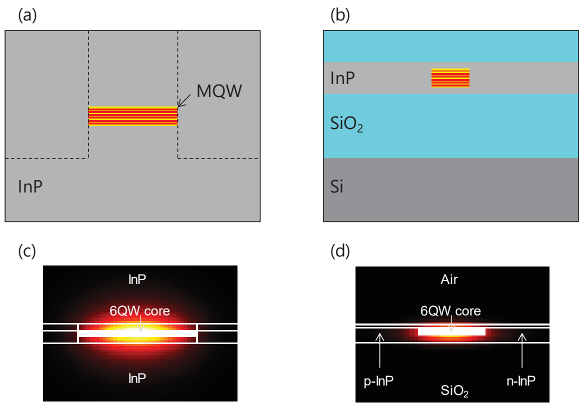

Fig. 1: Schematic cross sectional image of (a) conventional and (b) our membrane-based semiconductor lasers. Fundamental optical modes in (c) conventional and (d) our membrane-based semiconductor lasers.

Figure 1 shows the fundamental optical mode of conventional InP-based lasers and our membrane-based lasers. The conventional structure had Γ of 5.9% in multiple quantum wells (MQW). By using a membrane-based structure, it could be increased by up to 10.1% due to the very large refractive index contrast between SiO_2 and InP[5]. We were also able to reduce the width of the active region to less than 1 μm to reduce the active volume.

The membrane lasers and PhC lasers were fabricated in a similar manner. First, we grew an etch-stop layer and MQW sandwiched by thin InP layers on 2-inch InP wafers. The InP epitaxial wafers were bonded to thermally oxidized Si wafers by oxygen plasma assisted bonding. If Si waveguides were required, we bonded InP epitaxial wafers on silicon on insulator (SOI) wafers after the waveguide etching and surface planarization by SiO_2. Then the BH structures were formed by selective etching of MQW and regrowth. Lateral p-i-n junctions were formed by Si ion implantation and Zn diffusion.

Optical cavities were defined by electron beam lithography. To form surface gratings for the membrane lasers, the top InP layer was slightly etched using the grating patterns. To form PhC, the InP-based slabs were fully etched using the PhC hole patterns. After forming optical cavities, electrodes were deposited on top of the membrane layers by lift-off.

To obtain efficient optical coupling to fibres, we used spot-size converters (SSC) for the membrane lasers. The SiO_x or SiN dielectric optical waveguides were formed on the InP inverse-tapered waveguides so that the light emission from the InP was adiabatically coupled to the dielectric waveguides.

Device characteristics: membrane lasers

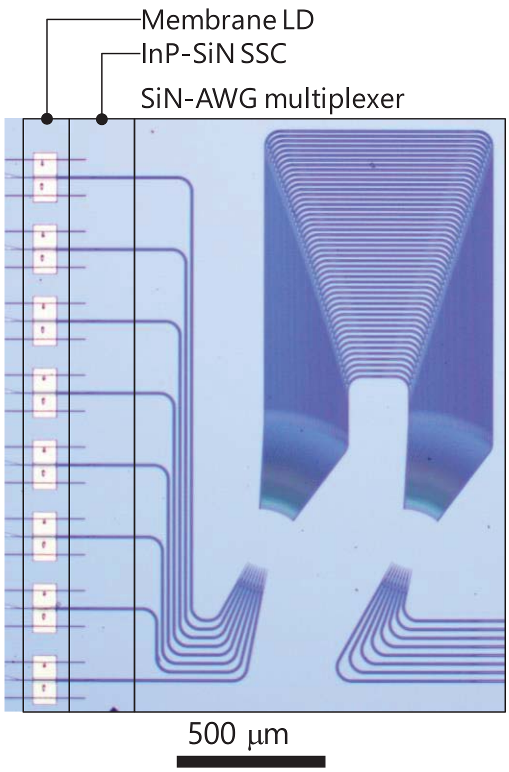

Fig. 2: Microscopic image of the fabricated 8-channel membrane lasers integrated with SiN-based AWG.

The lasing wavelength of the membrane lasers was determined by the surface grating, making it possible to make an array of multiple membrane lasers with different wavelengths. We used SiN with the dimensions 450 × 900 nm and designed compact arrayed waveguide gratings (AWGs)[6]. The AWG and 8-channel membrane lasers were monolithically integrated with a channel spacing of 380 GHz in the O-band. We used a high numerical-aperture fibre (HNAF) to obtain efficient optical coupling from dielectric waveguides. A picture of the fabricated membrane lasers is shown in Fig. 2.

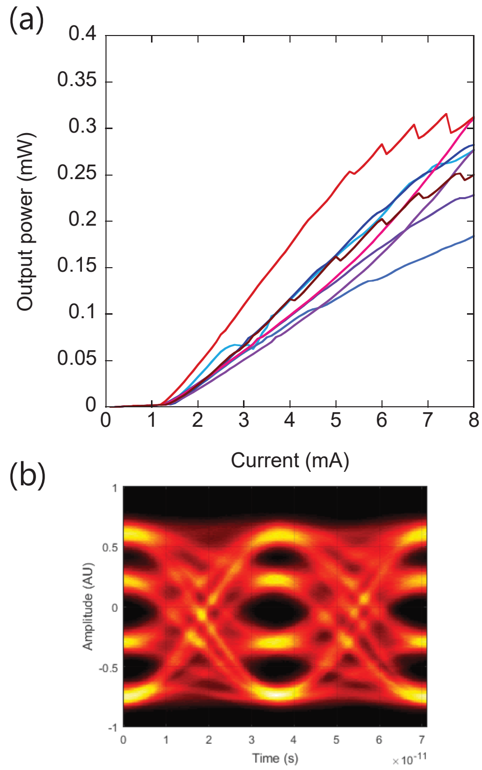

Fig. 3: (a) Output power of the 8-channel membrane lasers versus injected current. (b) Eye diagram of the channel 7 after nonlinear equalizer. The data format was 28 GBaud PAM-4.

Figure 3(a) shows the output power versus the current injected into the membrane lasers (I-L characteristics). All eight channels started lasing at a threshold current of 1.4 ± 0.1 mA. The dynamic characteristics of the membrane lasers were also evaluated. Figure 3(b) shows an eye diagram of the membrane laser operating at 56 Gbit/s PAM-4 after offline processing with a nonlinear equalizer. The bit error rate (BER) was smaller than 10^{-3} in this channel, and the total BER was 2.7×10^{-3}.

To relax the wavelength tolerance of the wavelength division multiplex (WDM) lasers, coarse WDM (CWDM) spacing is more effective than dense spacing. However, the emission wavelength of the MQW needs to be changed for each wavelength channel. We used the selective area growth of the MQW on 50-nm thick InP membrane on SiO_2/Si[7]. By optimizing the shape of the growth masks, we attained a photoluminescence peak wavelength controlled for a 40-nm wavelength range. The 8-channel CWDM membrane lasers were fabricated using this selective area growth, and we attained continuous-wave operation with a threshold current of approximately 3 mA. A 25.8-Gbit/s NRZ direct modulation was demonstrated for all eight channels.

We also designed laser drivers using CMOS-based analog circuits[8]. We designed single-end CMOS-based cascode shunt driver circuits. We located cascode-connected NMOS transistors in parallel with the DML. When a higher signal is applied to the NMOS transistor, the current to NMOS transistors increases so that the DML current decreases; the optical signal was the inverted logic of the input signal. We fabricated four channels of the drivers and DMLs and then connected them by flip-chip bonding. We drove the 4-channel drivers and DMLs at a signal of 25-Gbit/s NRZ waveform. The transmission of all four channels was error free over 2-km single mode fibre (SMF), and the total power consumption was only 137 mW, which corresponded to an energy cost of 1.37 pJ/bit.

Device characteristics: PhC lasers

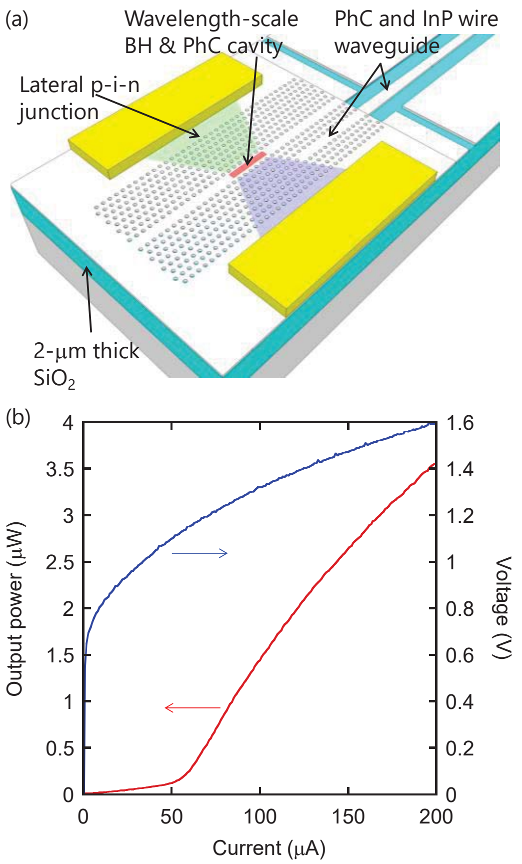

Fig. 4: (a) Schematic image of the LEAP lasers on InP substrates. (b) I-L characteristics of the LEAP lasers fabricated on Si substrates.

A schematic image of the fabricated PhC lasers on Si substrates are shown in Fig. 4(a). We refer to our developed lasers as lambda-scale embedded active region PhC (LEAP) lasers. After the first demonstration of continuous-wave electrically-driven LEAP lasers[9], we investigated reducing the threshold current and operating energy of the LEAP lasers. We demonstrated that a record low threshold current of 4.8 μA and operating energy of 4.4 fJ/bit were feasible at 10-Gbit/s operation[10]. However, these results were demonstrated on InP substrates; integration on Si substrates was still required to use LEAP lasers as light sources for on-chip optical interconnects.

We applied fabrication procedures to the LEAP lasers which were similar to the procedures for the membrane lasers and successfully demonstrated continuous-wave operation of the LEAP lasers on Si substrates[11]. Figure 4(b) shows an I-L characteristic of the LEAP lasers on Si. We attained a threshold current of 57 μA and a maximum output power of more than 3.5 μW. The LEAP lasers operated in a single mode with a lasing wavelength of 1554.2 nm.

The output light from the LEAP lasers was coupled to the InP channel waveguides. We were also able to obtain a light coupling to Si waveguides by replacing Si wafers with SOI wafers[12]. We attained continuous-wave operation of the LEAP lasers on Si waveguides with a threshold current of 24 μA. 10-Gbit/s direct modulation was also demonstrated with an energy cost of 7.3 fJ/bit.

Conclusion

In this paper, we reviewed our recent work on membrane lasers and PhC (LEAP) lasers. Both are based on the same concept of increasing the optical confinement factor and reducing the active volume, though on different scales. The threshold currents of the membrane lasers ranged from sub-mA to mA, while μA-scale threshold current was feasible for the LEAP lasers. Given these differences, the membrane lasers can be considered effective light sources for short-distance optical interconnects such as rack-to-rack or chip-to-chip. For optical interconnects for distances of cm, such as on-chip, LEAP lasers may be effective light sources due to their ultralow operating energy.

Acknowledgements

We would like to thank Mr. Y. Shouji, Y. Yokoyama, and K. Ishibashi for assistance in fabricating the devices.

References

[1] D. Kuchta, “High Speed VCSELs and Co-Packaging for Short Reach Communication within Cloud and High Performance Computing,” Proc. Microoptics Conference (MOC), paper. G-1, 2019.

[2] C. A. Thraskias et al., “Survey of Photonic and Plasmonic Interconnect Technologies for Intra-Datacenter and High-Performance Computing Communications,” IEEE Commun. Surveys & Tutorials, vol. 20, no. 4, pp. 2758-2783, 2018.

[3] D. A. B. Miller, “Device Requirements for Optical Interconnects to Silicon Chips,” Proc. IEEE, vol. 97, no. 7, pp. 1166-1185, 2009.

[4] S. Matsuo et al., “Ultralow Operating Energy Electrically Driven Photonic Crystal Lasers,” J. Sel. Top. Quantum electron., vol. 19, no. 4, pp.4900311, 2013.

[5] T. Fujii et al., “Heterogeneously Integrated Membrane Lasers on Si Substrate for Low Operating Energy Optical Links,” J. Sel. Top. Quantum Electron., vol. 24, no. 1, pp. 1500408, 2018.

[6] H. Nishi et al., “Integration of Eight-Channel Directly Modulated Membrane-Laser Array and SiN AWG Multiplexer on Si,” J. Lightwave Technol., vol. 37, no. 2, pp. 266-273, 2019.

[7] T. Fujii et al., “Wide-Wavelength Range Membrane laser Array Using Selectively Grown InGaAlAs MQWs on InP-on-insulator,” Proc. European Conf. on Optical Commun. (ECOC), paper Th.2.D.4, 2019.

[8] T. Kishi et al., “A 137-mW, 4 ch × 25-Gbps Low-Power Compact Transmitter Flip-Chip-Bonded 1.3-μm LD-Array-on-Si,” Prof. Optical Fiber Communications Conference and Exposition (OFC), paper. M2D.2, 2018.

[9] S. Matsuo et al., “Room-temperature continuous-wave operation of lateral current injection wavelength-scale embedded active-region photonic-crystal laser,” Optics Express, vol. 20, no. 4, pp. 3773-3780, 2012.

[10] K. Takeda et al., “Few-fJ/bit data transmissions using directly modulated lambda-scale embedded active region photonic-crystal lasers,” Nature Photonics, vol. 7, pp. 569-575, 2013.

[11] K. Takeda et al., “Photonic-crystal lasers on silicon for chip-scale optical interconnects,” Proc. Photonics West, Novel In-Plane Semiconductor Lasers XV, 976710, 2016.

[12] H. Nishi et al., “Low-Operating Energy Heterogeneously Integrated Photonic-Crystal Laser on Si Waveguide,” Proc. Intl. Semiconductor Laser Conf. (ISLC), paper TuB3, 2018.